

Bandwidth Improvement of Bowtie Antenna for GPR Applications Using Antipodal Technique, Corner Bending, and Triangular Slot Modifications

Osama Alali^{1, *}, Abdelrazak Badawieh¹, and Mohammad Alhariri²

Abstract—In this paper, the bandwidth of a bowtie antenna is improved to meet the requirements of Ground Penetrating Radar (GPR) applications that need a fractional bandwidth greater than 100% and are able to operate at low frequencies. This was done using several modification steps, which were the use of Antipodal technique for its advantages in reducing the complexity of the feeder network to achieve good matching with a standard 50-Ω SMA connector, bending the four corners of the arms, and adding a triangular slot in each arm. The simulation was carried out using CST Microwave Studio to study the effect of each modification step on improving the bandwidth. The simulation results of the new antenna achieved a fractional bandwidth of 138% within the frequency range (1–5.45) GHz at the values of return loss ($S_{11} \leq -10$ dB). The new antenna was also fabricated, and the return loss was measured and showed a good agreement with the simulation results.

1. INTRODUCTION

GPR systems are effective non-destructive tools which use transmission and reception of electromagnetic waves to detect targets under different surfaces such as ground, water, ice, cement, and other propagation media with different permittivities [1]. Antennas are an essential part of GPR systems, so they must be designed to meet the requirements of these systems, such as the ability to work at low frequencies to increase the depth of penetration and ability to work at high frequencies to achieve good resolution to distinguish small-sized targets. Therefore, the design and development of UWB antennas are necessary to increase the performance of GPR systems [2].

To classify systems according to their bandwidth, the fractional bandwidth (FBW) is defined by the relationship in Eq. (1). Antennas can be considered ultra-wideband if they achieve a fractional bandwidth of greater than 25% within the frequency range 3–11 GHz [3–5], but GPR systems require to achieve a fractional bandwidth greater than 100% [6], in addition to work at lower frequencies.

$$FBW = 2 \frac{f_h - f_l}{f_h + f_l} \times 100\% \quad (1)$$

where F_h is the higher frequency, and F_l is the lower frequency in the bandwidth.

Bowtie antenna is widely used in GPR systems [2] due to its positive features such as small size and weight, planar, low dispersion, low cost, good phase stability, easy modification, and easy fabrication [4]. However, the frequency bandwidth of the traditional bowtie antenna is not wide enough to be used for GPR applications, so many researches added several modifications to overcome this drawback using cutting edges of the arms [7, 8], rounding corners [9–11], resistive loading [6, 12–14], capacitive loading [6–10, 13, 15], antipodal technique [4, 7, 16–19], and self-complementary technique [3, 20].

Received 10 October 2021, Accepted 27 November 2021, Scheduled 8 December 2021

* Corresponding author: Osama Alali (osamaalimhn@gmail.com).

¹ Department of Communication Engineering, Damascus University, Damascus, Syria. ² Department of Communication Engineering, Higher Institute for Applied Science and Technology, Damascus, Syria.

In this paper, we will present a combination of several previous methods to study their impact on improving the bandwidth of the traditional bowtie antenna, to get a new UWB bowtie antenna with bandwidth greater than 100% that secures the requirements of GPR systems.

2. TRADITIONAL BOWTIE ANTENNA (TBA) DESIGN

TBA is formed from a two-dimensional geometric approximation of a biconical antenna, getting two symmetrical triangular arms on one plane [6, 21] with two coplanar striplines (CPSs) for feeding from a 50-Ω SMA connector as shown in Figure 1.

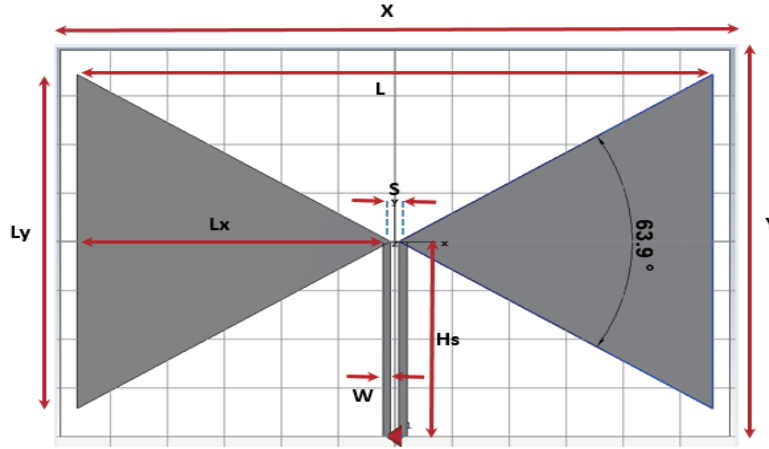


Figure 1. TBA (Traditional Bowtie Antenna).

In this design, an FR4 substrate with dielectric constant ($\epsilon_r = 4.3$), thickness ($h = 1.6$ mm), and loss tangent ($\delta = 0.025$) was used. The antenna dimensions shown in Table 1 were designed based on Equation (2) [5, 15] where λ is the wavelength for the minimum frequency f in the bandwidth which is 1 GHz in our design.

$$L = \frac{1.6\lambda_0}{\sqrt{\epsilon_r}} \quad (2)$$

The characteristic impedance Z of the TBA can be calculated from Equation (3) [6, 15, 21].

$$Z_0 = 120 \ln \left(\cot \frac{\theta}{4} \right) \quad (3)$$

where θ is the flare angle of the arms. Now TBA has $\theta = 63.9^\circ$ and $Z = 150 \Omega$.

Table 1. Dimensions of TBA parameters at $F = 1$ GHz.

Symbol	Parameter	Value [mm]
Lx	Arm Length	110
Ly	Arm Wide	137.2
L	Antenna Length	223
X	Substrate Length	235
Y	Substrate Wide	158.6
S	Gap	3
Hs	CPS Length	80
W	CPS Wide	2.8

In the case of direct connection with the 50-Ω SMA connector ignoring the matching, the work of the TBA will not be acceptable, but in the case of ideal connection with a 150-Ω virtual connector, the ideal-TBA will operate within the frequency range (1.25–5.87) GHz for return loss values ($S_{11} \leq -10$ dB). Figure 2 shows the simulation results of the reflection coefficient S_{11} for the previous two cases using CST Microwave Studio.

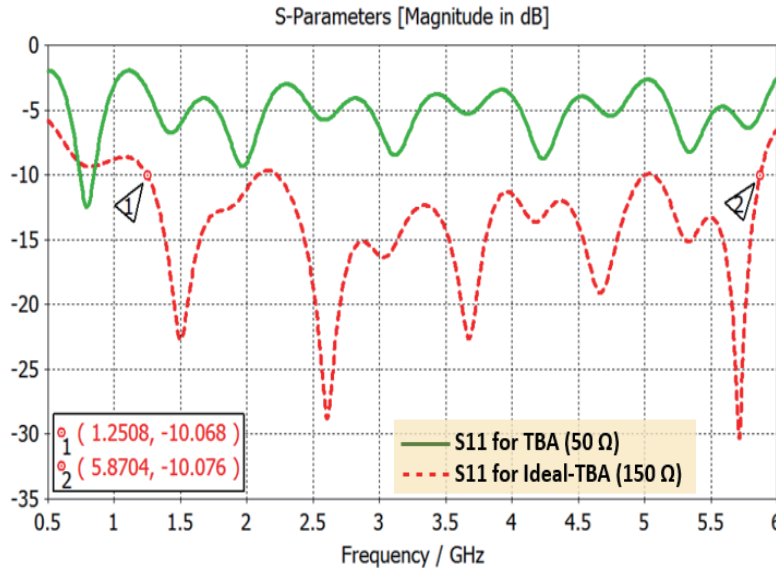


Figure 2. Matching effect on TBA and ideal-TBA bandwidth.

Practically, TBA needs a good matching between 150 Ω and 50 Ω. This can be achieved by adding a feeder network as a Microstrip to CPS transition [21, 22], but that will lead to a reduction in bandwidth, increasing antenna size and design complexity [3].

The proposed solution to overcome this problem is to use antipodal technique, which increases the ability of TBA for matching without the need of this type of feeder network, thus eliminating the limited bandwidth and increasing the possibility of applying the modifications in practical cases.

3. PROPOSED MODIFICATIONS FOR BANDWIDTH IMPROVEMENT

3.1. Antipodal Technique

To apply the antipodal technique on the TBA, one of the arms and its feed line were moved from the front side to the back side of the substrate [16]. The bandwidth of Antipodal Traditional Bowtie Antenna (A-TBA) had a perfect agreement with the bandwidth of TBA as shown in Figure 3.

The antipodal technique now allows for an adjustment of the gap between the arms where the arms can be closer and overlapped in a way that could not be done in TBA with its CPS to achieve the desired matching.

By the simulation of return loss of A-TBA (50 Ω) for several fixed values of the gap S where $S = -2, -1, 0, 1, 2, 3$, Figure 4 shows that none of these fixed values of the gap achieves the correct work of the antenna. Therefore, the proposed solution was to use decreasing values of the gap from $S_{\text{start}} = 1.8$ mm at the beginning of the arms to $S_{\text{end}} = 0$ mm within a region that can be called (Tapered Gap) by converting the two feed lines to two tapered lines that meet oppositely on both sides at 50-Ω port as shown in Figure 5. Now this antenna is called A-TGBA (Antipodal Tapered Gap Bowtie Antenna).

The minimum width of the feeding line is 0.5 mm at the arm, and the maximum is 4.8 mm at the port. This feeder network achieved the matching with 50-Ω port in the real part impedance as shown in Figure 6 all over the bandwidth without the need for any additions that may increase the antenna size.

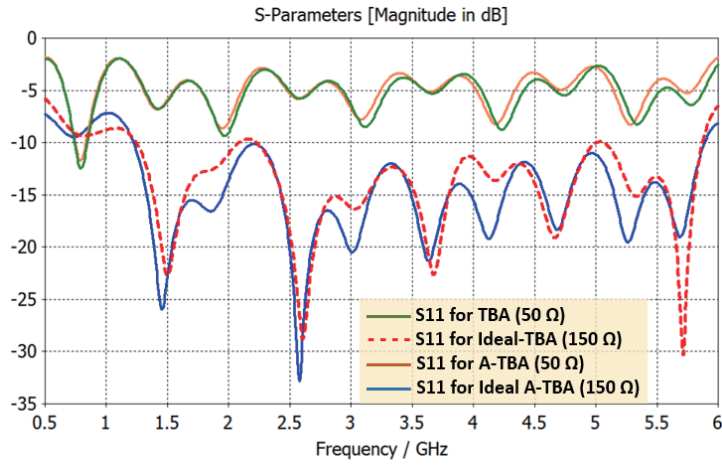


Figure 3. S_{11} parameter comparison between TBA & A-TBA.

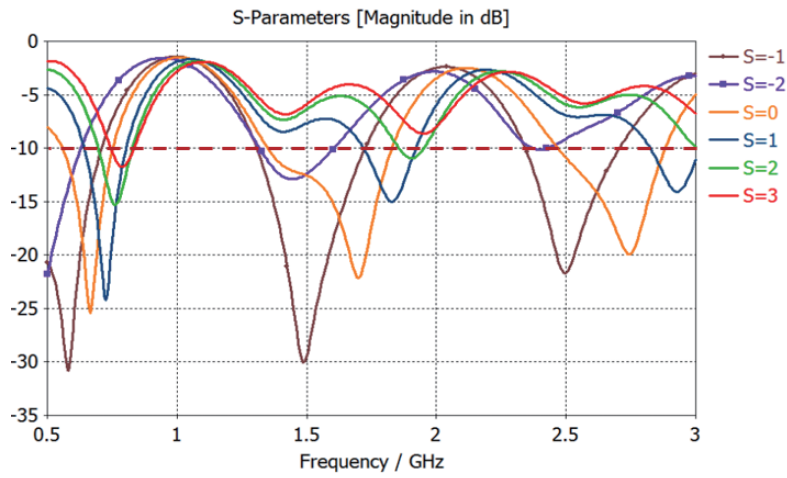


Figure 4. Return loss simulation results for A-BTA ($50\ \Omega$) with several fixed gap values.

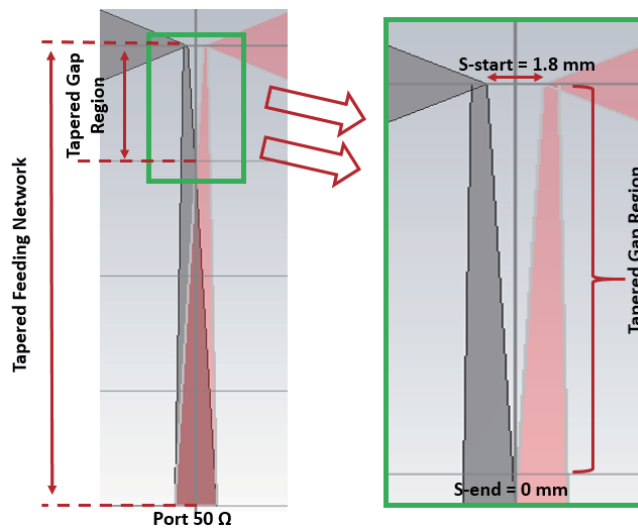


Figure 5. Tapered gap using tapered feeder network.

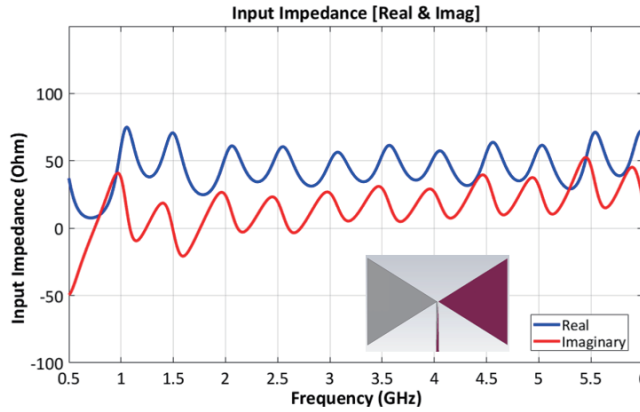


Figure 6. Real & imaginary part input impedance for A-TGBA.

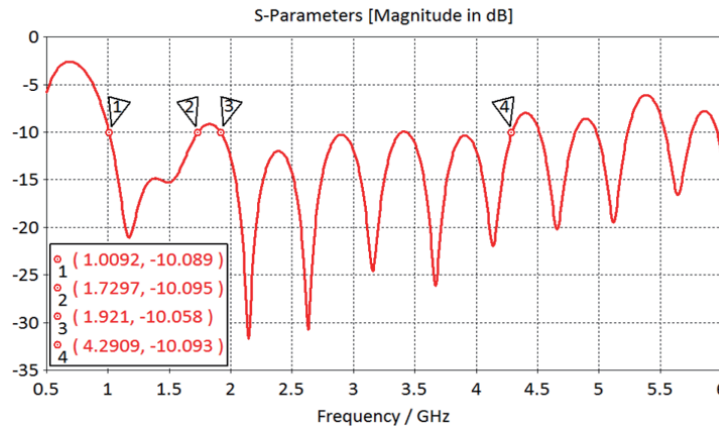


Figure 7. Return loss for A-TGBA.

Simulation results of the reflection coefficient of the A-TGBA show that it operates in the frequency range (1–4.29) GHz with frequency notch at (1.73–1.92) GHz and has S_{11} greater than -10 dB as shown in Figure 7.

3.2. Corner Bending

The proposed modification here is to use bending of the four corners of the triangular arms to reduce the reflection of the power [11], which leads to an additional increase in the bandwidth of the antenna, called now Antipodal Bended Bowtie Antenna (A-BBA).

For several values of the corner bending radius ($B = 0, 10, 20, 30$ mm), return loss simulation results of the A-BBA show that the notch was eliminated and became below -10 dB as shown in Figure 8. A-BBA worked within the bandwidth (1–5.24) GHz at $B = 20$ mm which was a suitable choice.

3.3. Triangular Slot Loading

A triangular slot was added in each arm as shown in Figure 9(a) to form a new antenna called Antipodal Slot Bended Bowtie Antenna (A-SBBA). Return loss simulation results in Figure 10 show an additional improvement in the bandwidth, where A-SBBA worked within the bandwidth of (1–5.45) GHz at ($S_{11} \leq -10$ dB) with a fractional bandwidth of 138%. After testing several slot dimensions, the best one had the dimensions shown in Figure 9(b). It can be clearly noticed that the bandwidth of the A-SBBA is similar to the previous ideal-TBA assumption and shown in Figure 2 achieving better reflection coefficient values and lower frequency, which is better for GPR applications.

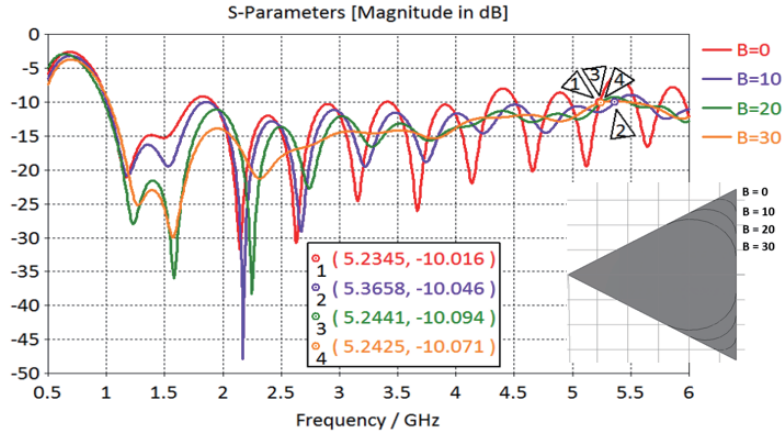


Figure 8. A-BBA bandwidth.

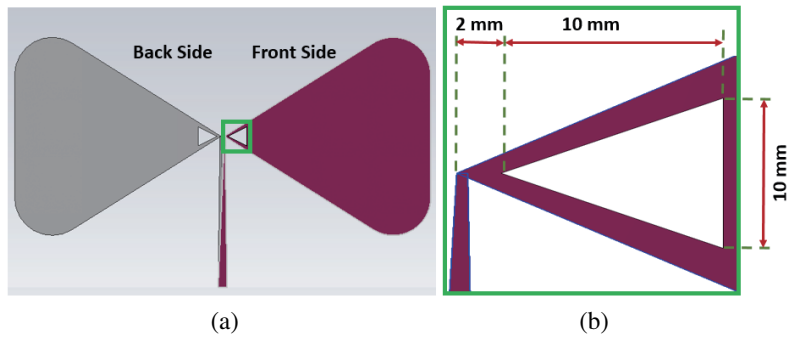


Figure 9. (a) A-SBBA geometry. (b) Triangle slot dimensions.

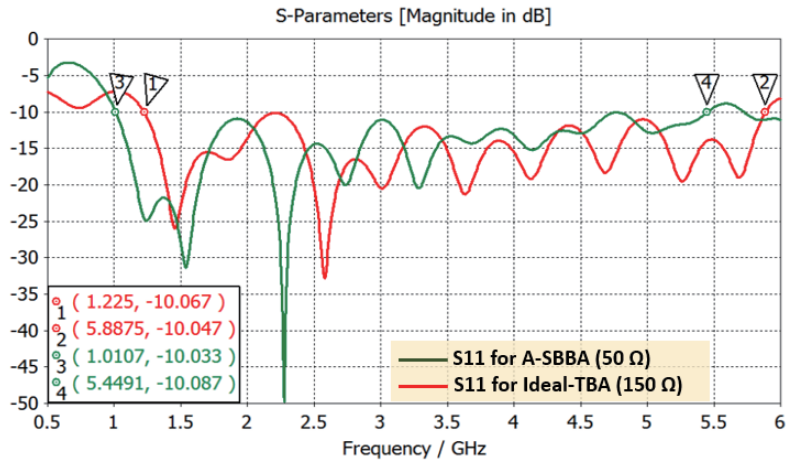


Figure 10. Comparison between A-SBBA and ideal-TBA bandwidth.

The radiation efficiency of A-SBBA is (60–97)%, and the gain is (2.2–4.2) dB for the overall frequency range. The three-dimensional radiation pattern of the A-SBBA was compared with the Ideal-TBA at the frequency 1.5 GHz. Figure 11 shows a very good agreement between them with a slight decrease in the directivity of the A-SBBA due to the bended corners. The A-SBBA achieves a maximum directivity of 4.24 dBi towards the direction of the earth in GPR applications, while the maximum directivity for the ideal-TBA was 4.52 dBi, and maximum gain was for the same direction.

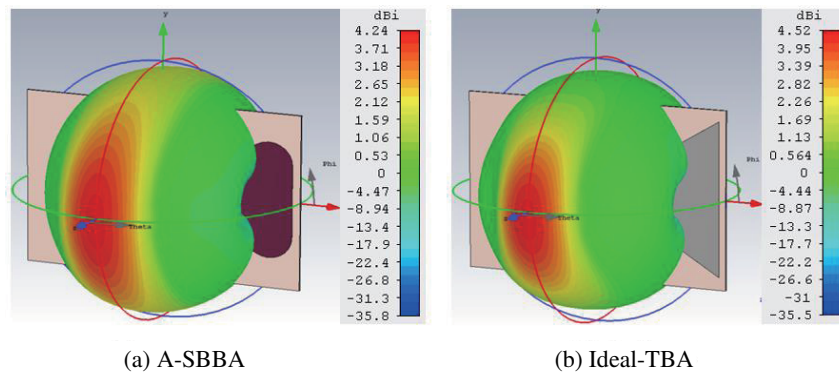


Figure 11. 3D Radiation pattern at F=1.5 GHz (a) for A-SBBA, (b) for Ideal-TBA.

4. RESULTS AND DISCUSSION

The new antenna (A-SBBA) was fabricated as shown in Figure 12. The return loss was measured using a ROHDE & SCHWARZ FSH20 vector Network Analyzer. Figure 13 shows that the antenna bandwidth at $S_{11} \leq -10$ dB operated within (1–6) GHz, so it achieved 142.8% fractional bandwidth in good agreement with the simulation results, which was 138%.

The simulation and implementation results can be summarized in Table 2, which shows the effect of each modification step performed in this paper on the bowtie antenna bandwidth.

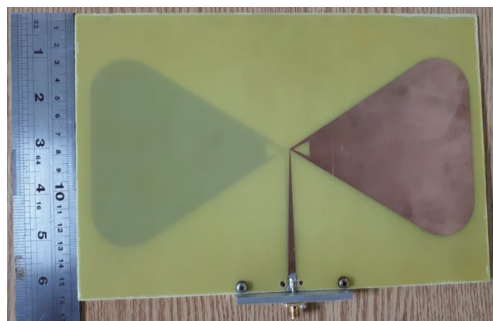


Figure 12. A-SBBA fabrication.

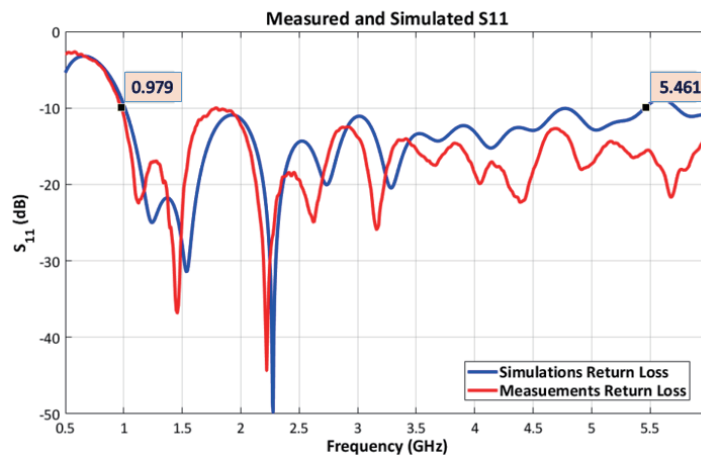


Figure 13. Bandwidth comparison between simulation and measurement results for A-SBBA.

Table 2. The effect of modifications on bowtie antenna bandwidth.

Antenna Type	Bandwidth GHz for $S_{11} \leq -10$ dB	Fractional Bandwidth (FBW) %
Ideal-TBA (150 Ω)	1.25–5.87	129.7%
TBA (50 Ω)	×	×
Ideal A-TBA (150 Ω)	1.25–5.87	129.7%
A-TBA (50 Ω)	×	×
A-TGBA	1–4.29 With Notch (1.73–1.92)	124.4% Ignoring the notch
A-BBA	1–5.24	135.9%
A-SBBA	1–5.45	138%
Fabricated A-SBBA	1–6	142.8 %

Table 3 shows a comparison of the bandwidth achieved in this work with other works done to improve the bandwidth of the bowtie antenna.

Table 3. Comparison between previous works and this work.

Ref	Using Techniques for Bowtie Antenna	Simulated BW in GHz	Simulated FBW %	Measured BW in GHz	Measured FBW %
[6] 2019	Lumped resistive loading, capacitive loading, cutting edges and cavity reflector.	0.64–2	103%	0.64–2.2	109%
[7] 2017	Double-sided arms and rectangular slots.	2–5	85.7%	2–5	85.7%
[8] 2011	CPW-Fed, slot arms with sharp corners and two metal stubs.	0.4–1.5	115.8%	0.4–1.5	115.8%
[9] 2016	Similar to Ref. [8] but using rounded corners and resistivity loading by graphite sheet.	1.3–4.5	110%	–	–
[14] 2016	Resistive loading and Metamaterial Lens.	0.3–3	163.6%	0.3–3	163.6%
[20] 2018	Self-complementary.	0.98–4.5	128.5%	0.98–4.5	128.5%
This work	Antipodal technique, bended corners and triangular slot.	1–5.45	138%	1–6	142.8%

We find that our design, which is characterized by simplicity, has achieved better fractional bandwidth than most of them except [14] which made its improvement in complexity.

5. CONCLUSION

In this paper, the bandwidth of a bowtie antenna was improved for GPR applications using antipodal technique, corner bending, and a triangular slot in each arm. The effect of each modification step on improving the bandwidth was investigated, and finally a new antenna was obtained that achieved a fractional bandwidth of 138% within the frequency range (1–5.45) GHz that is suitable for GPR systems. The new antenna was fabricated, and return loss was measured. The fabricated antenna (A-SBBA) worked in the frequency range (1–6) GHz with a fractional bandwidth of 142.8%. The effect of the modifications on the electrical and radiation characteristics of this antenna will be the focus of research in future work.

REFERENCES

1. Rhee, J. Y., K. T. Park, J. W. Cho, and S. Y. Lee, "A study of the application and the limitations of GPR investigation on underground survey of the Korean expressways," *Remote Sensing*, Vol. 13, No. 9, 1805, May 2021.
2. Nayak, R. and S. Maiti, "A review of bow-tie antennas for GPR applications," *IETE Technical Review*, Vol. 36, No. 4, 382–397, Jul. 2019.
3. Sayidmarie, K. H. and Y. A. Fadhel, "A planar self-complementary bow-tie antenna for UWB applications," *Progress In Electromagnetics Research C*, Vol. 35, 253–267, 2013.
4. Dadgarpour, A., G. Dadashzadeh, M. Naser-Moghadasi, and F. Jolani, "Design and optimization of compact balanced antipodal staircase bow-tie antenna," *Antennas Wirel. Propag. Lett.*, Vol. 8, 1135–1138, 2009.
5. Ali, J., N. Abdullah, M. Yusof, E. Mohd, and S. Mohd, "Ultra-wideband antenna design for GPR applications: A review," *IJACSA*, Vol. 8, No. 7, 2017.
6. Wu, Y., F. Shen, Y. Yuan, and D. Xu, "An improved modified universal ultra-wideband antenna designed for step frequency continuous wave ground penetrating radar system," *Sensors*, Vol. 19, No. 5, 1045, Mar. 2019.
7. Ting, J., D. Oloumi, and K. Rambabu, "A miniaturized broadband bow-tie antenna with improved cross-polarization performance," *AEU — International Journal of Electronics and Communications*, Vol. 78, 173–180, Aug. 2017.
8. Sagnard, F. and F. Rejiba, "Wide band coplanar waveguide-fed bowtie slot antenna for a large range of ground penetrating radar applications," *IET Microw. Antennas Propag.*, Vol. 5, No. 6, 734, 2011.
9. Nayak, R., S. Maiti, and S. K. Patra, "Design and simulation of compact UWB Bow-tie antenna with reduced end-fire reflections for GPR applications," *2016 International Conference on Wireless Communications, Signal Processing and Networking (WiSPNET)*, 1786–1790, Chennai, India, Mar. 2016.
10. Awl, H. N., et al., "Bandwidth improvement in bow-tie microstrip antennas: The effect of substrate type and design dimensions," *Applied Sciences*, Vol. 10, No. 2, 504, Jan. 2020.
11. Qu, S. and C. L. Ruan, "Effect of round corners on bowtie antennas," *Progress In Electromagnetics Research*, Vol. 57, 179–195, 2006.
12. Shao, J., G. Fang, Y. Ji, and H. Yin, "Semicircular slot-tuned planar half-ellipse antenna with a shallow Vee-cavity in vital sign detection," *IEEE J. Sel. to Appl. Earth Observations Remote Sensing*, Vol. 7, No. 3, 767–774, Mar. 2014.
13. Marsh, L. A., et al., "Combining electromagnetic spectroscopy and ground-penetrating radar for the detection of anti-personnel landmines," *Sensors*, Vol. 19, No. 15, 3390, Aug. 2019.
14. Ajith, K. K. and A. Bhattacharya, "Printed compact lens antenna for uhf band applications," *Progress In Electromagnetics Research C*, Vol. 62, 11–22, 2016.
15. Li, K., T. Dong, and Z. Xia, "Improvement of bow-tie antenna for ground penetrating radar," *2019 International Conference on Microwave and Millimeter Wave Technology (ICMMT)*, 1–3, Guangzhou, China, May 2019.

16. Vijayalakshmi, J. and G. Murugesan, "Improved bandwidth and gain in ultra-wideband staircase antipodal bowtie antenna with rounded edge for microwave imaging applications," *Appl. Math. Inf. Sci.*, Vol. 12, No. 6, 1197–1202, Nov. 2018.
17. Dastranj, A., "Design and implementation of a compact super-wideband printed antipodal antenna using fractal elements," *Journal of Communication Engineering*, Vol. 7, No. 1, 12, 2018.
18. Ganguly, D., Y. M. M. Antar, A. Somagani, and C. Saha, "Design of an antipodal bowtie array MIMO antenna for 5G mobile applications," *2019 IEEE International Symposium on Antennas and Propagation and USNC-URSI Radio Science Meeting*, 421–422, Atlanta, GA, USA, Jul. 2019.
19. Li, M., C. Domier, X. Liu, and N. C. Luhmann, "Wide band MM-wave, double-sided printed bowtie antenna for phased array applications," *2015 IEEE International Symposium on Antennas and Propagation & USNC/URSI National Radio Science Meeting*, 2063–2064, Vancouver, BC, Canada, Jul. 2015.
20. Joula, M., V. Rafiei, and S. Karamzadeh, "High gain UWB bow-tie antenna design for ground penetrating radar application," *Microw. Opt. Technol. Lett.*, 2018.
21. Balanis, C. A., *Antenna Theory Analysis and Design*, 4th Edition, Wiley, 2016.
22. Woo, D. S., Y. K. Cho, and K. W. Kim, "Balance analysis of microstrip-to-CPS baluns and its effects on broadband antenna performance," *International Journal of Antennas and Propagation*, Vol. 2013, 1–9, 2013.